THE JOURNAL OF PHYSICAL CHEMISTRY C

Article

pubs.acs.org/JPCC

Reaction of CO, CH_2O, CH_3OH on Zn-Modified Pt(111) Surfaces

Eddie Martono and John M. Vohs*

Department of Chemical and Biomolecular Engineering, University of Pennsylvania, Philadelphia, Pennsylvania 19104, United States

ABSTRACT: In order to provide insight into how alloying Pt with Zn affects its reactivity for the steam reforming of methanol (SRM), the adsorption and reaction of CO, CH_2O, and CH_3OH on Zn-modified Pt(111) surfaces was investigated using a combination of X-ray photoelectron spectroscopy (XPS), high resolution electron energy loss spectroscopy (HREELS), and temperature-programmed desorption (TPD). The reactivity of PtZn near surface alloys were found to be similar to that of Pt(111) and have relatively low activity for methanol decomposition. In contrast, on Zn-modified Pt(111) surfaces where the Zn was present only as adatoms, methanol adsorbs dissociatively to form methoxide groups bound to both Pt and Zn sites. The Pt-bound methoxides are stable up to ~450 K at which point they undergo dehydrogenation to produce H_2 and CO, while those adsorbed on Zn sites undergo partial dehydrogenation at 300 K to produce formaldehyde which desorbs intact. These differences in the reactivity of the two types of surfaces studied suggest that Zn adatoms may play a role as active sites for the SRM reaction which is in agreement with studies of high surface area PtZn catalysts that indicate that excess surface Zn is required to obtain high selectivity to CO_2 and H_2.

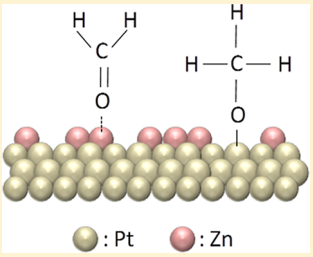

INTRODUCTION

The efficient production of high-purity H_2 remains a significant challenge to the adoption of fuel cells as an environmentally friendly electricity generation technology.[1,2] Currently the majority of the H_2 used industrially is produced from natural gas through a multistep steam reforming process that also produces CO_2.[3,4] To decrease net CO_2 emissions it would be desirable to produce H_2 from more renewable resources, such as, biomass-derived alcohols or polyols. This has motivated research into the development of highly active and selective catalysts for alcohol steam reforming (e.g., $CH_3OH + H_2O \rightarrow 3H_2 + CO_2$).[5−12] For methanol reforming, Cu supported on ZnO is the current state of the art catalyst.[13−15] Despite its high activity and selectivity to H_2 and CO_2, Cu/ZnO has several drawbacks including being pyrophoric once reduced and a high propensity for sintering at relatively mild operating temperatures.[16,17] This has motivated the search for an alternate catalyst with bimetallics containing a group 10 metal, such as, Pt or Pd, emerging as leading candidates. Takezawa and Iwasa have shown that when these metals are alloyed with Zn they exhibit activity and selectivity for the steam reforming of methanol (SRM) comparable to that of Cu/ZnO and are less prone to deactivation.[6,18−20] They also have attractive properties as catalysts for ethanol steam reforming.

The role of Zn in these catalysts is particularly interesting since it has a very dramatic effect on selectivity. For example, the CO/CO_2 selectivity for SRM changes from greater than 85% CO for both Pt and Pd on inert supports such as SiO_2, to greater than 95% CO_2 when these metals are supported on ZnO.[19] In the latter case, it has been shown that under reaction conditions the metals become alloyed with Zn provided via reduction of the support.[18] These observations have motivated numerous fundamental theoretical and experimental studies of the mechanism by which alloying with Zn affects the reactivity of the Group 10 metals,[20−29] with most of this work focusing on the PdZn system. In studies of Zn-modified Pd(111) surfaces Jeroro and Vohs showed that one effect of Zn addition was to increase the barriers for C−H bond scission in adsorbed methoxide and formaldehyde intermediates, thereby stabilizing these species from rapid dehydrogenation to CO as occurs on the Zn-free Pd surface.[23] Similar results have been reported in studies of the reaction of methanol on multilayer PdZn alloy films grown on Pd(111).[30] Both theoretical and experimental studies have also shown that addition of Zn to Pd alters the density of states (DOS) near the Fermi energy causing the Pd 4d band to shift to higher binding energies compared to pure Pd making the DOS closely resemble that of Cu.[31−33] Thus, adding Zn to Pd makes the Pd appear more "Cu-like" resulting in a shift in the SRM selectivity toward the production of CO_2 and H_2 rather than CO and H_2

While similar reactivity trends are observed for the PdZn and PtZn systems,[6,20] relatively few fundamental studies of the effect of the addition of Zn to Pt on SRM activity have appeared in the literature.[25,28,34,35] Rodriguez et al. have shown, however, that like PdZn, alloying Pt with Zn causes the metal d-band to shift to higher energies, thereby making the valence band electronic structure of the alloy more similar to that of Cu.[28,34,36] In order to provide additional insight into how the addition of Zn to Pt affects its activity for SRM, in the work reported here, we have expanded our previous studies of the effect of alloying group 10 metals with Zn on their reactivity toward methanol to include the Pt−Zn system. In particular we have used XPS, TPD, and HREELS to study the adsorption and reaction of methanol, formaldehyde, and carbon monoxide on model catalysts consisting of Zn-modified Pt(111) and near-surface PtZn alloys on Pt(111).

Received: January 23, 2013
Revised: March 6, 2013
Published: March 14, 2013

   dx.doi.org/10.1021/jp400798q | J. Phys. Chem. C 2013, 117, 6692−6701

EXPERIMENTAL SECTION

Experiments were performed in two separate ultra high vacuum (UHV) chambers; both with a 2×10^{-10} Torr background pressure. Both chambers were equipped with an ion sputter gun (Physical Electronics) for sample cleaning and a quartz crystal microbalance (QCM, Inficon) for monitoring the flux from a Zn deposition source. The first chamber had a capability to perform XPS with the set up consisting of a hemispherical electron energy analyzer (Leybold-Heraeus) and a Mg Kα X-ray source (VG Microtech), while the second chamber was equipped with an HREEL spectrometer (LK Technologies). HREEL spectra were obtained using a 4 eV electron beam directed 60° with respect to the surface normal. The typical full width half-maximum (fwhm) for the HREEL elastic peak after tuning was approximately 40 cm^{-1}.

The Pt(111) single crystal (Goodfellow) was cleaned by cycles of ion sputtering with 2 kV Ar^+ for 30 min and annealing at 1100 K for 30 min. This procedure typically removed the majority of impurities leaving only a small amount of carbon on the surface which was removed using cycles of annealing in 2×10^{-9} Torr of O_2 for 30 min followed by annealing in vacuum until no carbon was detected by XPS or AES. The sample was mounted using 0.25 mm diameter Ta wires (Alfa Aesar, 99.9%) that were attached to the sample manipulator on the UHV chamber. The sample was heated resistively (3 K/s heating rate) and cooled to ~100 K via conduction from a liquid N_2 reservoir. Samples were exposed to adsorbates, CH_3OH (Fischer Scientific, 99.9%), O_2 (Matheson, 99.997%), and CO (Matheson, 99.9%), through a dosing needle with the sample positioned directly in front to maintain a low base pressure. CH_2O was produced through heating a tube containing solid paraformaldehyde (Fischer Scientific, 95%) to induce depolymerization. The enhancement factor of 100-fold measured previously due to direct dosing was factored into all doses reported.

Zn was deposited onto the Pt(111) surface using an evaporative Zn source consisting of a Zn wire (Alfa Aesar, 99.99%) wrapped around a 0.2 mm diameter W (Alfa Aesar, 99.95%) filament. The W filament was attached to an electrical feedthrough on the UHV system and heated resistively with the flux being monitored by the QCM. In this paper, Zn coverage is reported as effective monolayers where one monolayer was assumed to be 1.51×10^{15} atom/cm^2 which is the density of Pt atoms on the Pt(111) surface. Zn deposition was carried out with the Pt(111) sample held at or below 300 K. For these conditions the Zn remains adsorbed on the Pt(111) surface, and we refer to these as Zn/Pt(111) samples throughout the remainder of the paper. It has previously been shown that annealing monolayer and submonolayer Zn films on Pt(111) to 600 K induces reaction of the Zn with the Pt to form an alloy.[34,35] Since multilayer Zn desorbs at ~500 K, this method for producing a PtZn alloy on the Pt(111) surface is somewhat self-limiting. Similar phenomenon has previously been reported for Zn/Pd(111), where the multilayer Zn desorption peak was observed at temperatures below 600 K and the Zn desorption associated with the PdZn alloy occurred at temperatures above 750 K.[37] Low energy ion scattering (LEIS) studies have shown that upon annealing to 600 K the Zn becomes distributed in the first 3−4 atomic layers, with the concentration of Zn in the surface layer being only 0.05 atomic %.[35] We use PtZn/Pt(111) to refer to these surface alloy samples throughout the remainder of the paper. Figure 1 shows a schematic diagram of the two types of Zn-modified Pt(111) samples that were used in this study.

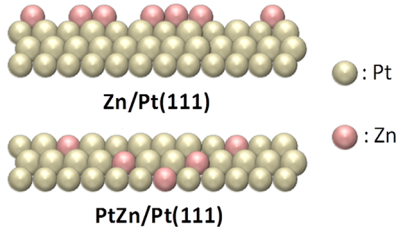

Figure 1. Models depicting the structure of the Zn/Pt(111) and PtZn/Pt(111) surfaces.

RESULTS

Figure 2 displays TPD data obtained from PtZn/Pt(111) surfaces dosed with 2 L of CH_3OH at 100 K as a function of the initial Zn coverage used during alloy synthesis. The bottom spectra in this figure correspond to the clean Pt(111) surface. These data show that Pt(111) is relatively unreactive toward CH_3OH with most of the CH_3OH desorbing intact in peaks centered at 150 and 195 K which can be attributed to desorption from multilayers and the first monolayer, respectively.[38−40] A small amount of CO and H_2 were also produced on the Zn-free surface at 350 and 480 K, respectively, but blank experiments indicate that this was due primarily to the adsorption of these molecules from the background gas in the vacuum chamber. These results are consistent with previous studies of the reaction of CH_3OH on Pt(111) where it has been shown that reaction occurs only at defect and step edge sites.[40−42] The data in Figure 2 also show that PtZn/Pt(111) alloy surfaces that were prepared using up to 0.6 ML of Zn were all similar and only slightly more active than the clean surface for the dehydrogenation of CH_3OH to produce CO and H_2. The small shift to lower temperatures that is apparent for both the CO and H_2 peaks indicates that Zn in the first layer slightly destabilizes the bonding of CO and H to the surface. This is consistent with previously reported CO TPD studies with PtZn/Pt(111) samples.[34−36] For initial Zn coverages >0.6 ML the PtZn/Pt(111) surface was found to be nearly unreactive toward methanol in comparison.

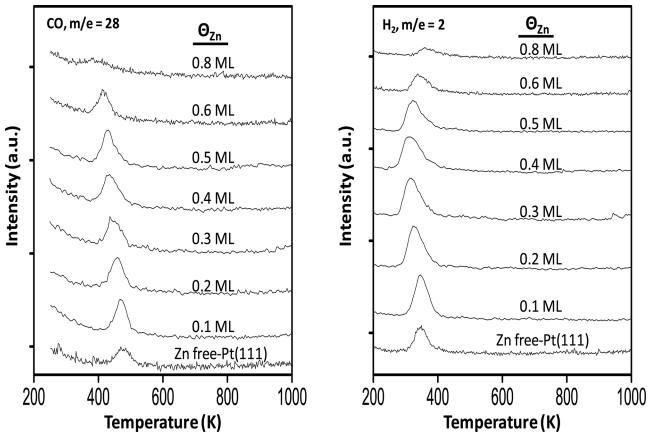

Figure 2. TPD spectra obtained following 2 L of CH_3OH dose at 100 K on PtZn/Pt(111) surfaces as a function of the Zn coverage used during alloy formation.

dx.doi.org/10.1021/jp400798q | J. Phys. Chem. C 2013, 117, 6692−6701

More interesting chemistry was observed for Zn/Pt(111) samples for which Zn was present only in the form of adatoms. Figure 3(a) shows the TPD results for a 0.4 L CO dose at 100 K as a function of the Zn adatom coverage. This CO dosage was chosen because previous studies have shown that CO preferably binds on atop sites at coverages below 0.2 ML, while bridge sites become populated at higher coverages. On the Zn-free Pt(111) surface, CO desorbed in a broad peak at 470 K, which is consistent with that reported in the literature for atop CO.[43] Addition of 0.1 ML of Zn to the Pt(111) surface prior to dosing CO resulted in a upward shift of the CO desorption temperature to 497 K. Further increases in the amount of adsorbed Zn up to 0.8 ML did not cause any additional shift in the CO desorption temperature, however, the area of the CO desorption peak decreased with increasing Zn coverage, disappearing altogether for 0.8 ML of Zn. CO is known to bond very weakly to Zn, desorbing below 125 K from Zn surfaces.[44−46] Thus, the decrease in the CO peak area with increasing Zn coverage can simply be attributed to Zn blocking the Pt adsorption sites. HREELS was used to measure the frequency of ν(CO) stretching mode of adsorbed CO and it was found to be 2080 cm^{-1} and invariant with Zn coverage. This frequency is consistent with that reported in the literature for CO adsorbed on atop Pt sites and demonstrates the Zn does not induce a change in the CO adsorption geometry (e.g., it does not shift to bridge sites).

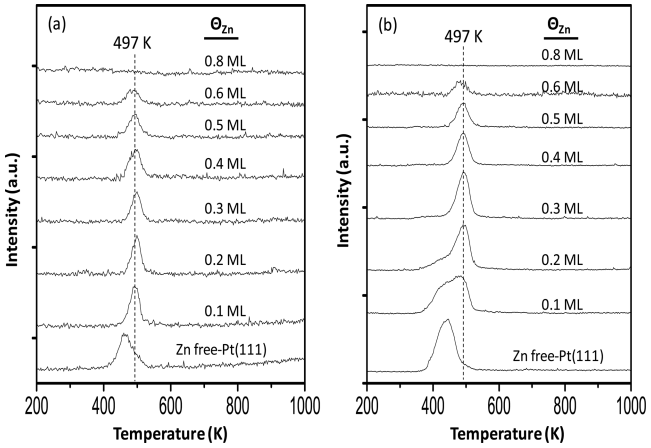

Figure 3. TPD spectra obtained following (a) 0.4 L and (b) 2 L CO dose at 100 K on Zn/Pt(111) as a function of the Zn adatom coverage.

It is interesting that for only 0.1 ML of Zn all of the adsorbed CO is stabilized relative to Zn-free Pt(111). Since the Zn does not induce a change in the adsorption site, the stabilization of the adsorbed CO by Zn must be due to an electronic effect. It is difficult to discern if this effect is local to the Zn adatoms or longer range from the low CO coverage (~0.2 ML) data in Figure 3a, since even for the low Zn coverages all of the adsorbed CO could populate Pt sites adjacent to Zn atoms. Additional insight is provided, however, by the CO TPD data as a function of Zn coverage in Figure 3b in which a higher 2 L CO dose was used. Note that in this case the peak indicative of CO on atop sites on clean Pt(111), decreases with increasing Zn adatom coverage up to 0.3 ML of Zn, while that of the Zn-stabilized species at 497 K exhibits behavior similar to that in the lower CO coverage experiments; i.e., it appears for 0.1 ML of Zn and then decreases in intensity with increasing Zn coverage. These results are consistent with the Zn stabilizing the adsorbed CO via a relatively short-range electronic effect.

As shown in Figure 4 which displays TPD spectra obtained following a 2 L of CH_3OH dose on Zn/Pt(111) as a function of the Zn coverage, the Zn adatoms also had a dramatic effect on the surface chemistry of CH_3OH. As noted above, the clean Pt(111) surface exhibits low reactivity toward CH_3OH with multilayer (154 K) and monolayer (195 K) molecular CH_3OH being the primary desorption products from this surface. Adding Zn to the surface, however, creates sites that are active for methanol dehydrogenation as signified by the disappearance of the molecularly adsorbed CH_3OH peak at 195 K, and the appearance of the reaction products, H_2, CO, and CH_2O. For 0.1 ML of Zn, CO desorbed in a broad peak at 480 K, while two H_2 desorption peaks were observed at 320 K (β_1) and 400 K (β_2). Increasing the Zn coverage to 0.2 ML resulted in the β_1 and β_2 H_2 peaks shifting to 295 and 450 K, respectively, and the emergence of a CH_2O peak at 438 K. The CO desorption feature can also now be resolved into two separate peaks at 438 K (α_1) and 497 K (α_2).

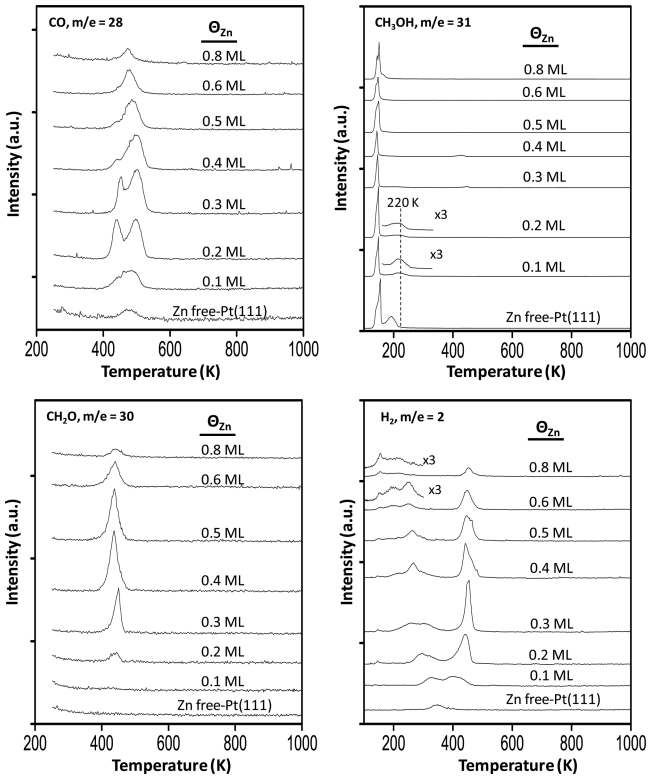

Figure 4. TPD spectra obtained following a 2 L of CH_3OH dose at 100 K on Zn/Pt(111) as a function of the Zn coverage.

For 0.2 ML of Zn/Pt(111) the α_1 and α_2 CO peaks were of nearly equal intensity. With increasing Zn coverage the areas of these peaks decreased with the α_1 peak disappearing for Zn coverages >0.5 ML and the α_2 persisting up to 0.8 ML. The CH_2O peak at 438 K, which emerged at 0.2 ML of Zn, peaked in intensity at 0.5 ML of Zn and then decreased significantly for higher Zn coverages. More complex behavior with Zn coverage was observed for the H_2 desorption features. Increasing the Zn coverage to 0.3 ML caused significant broadening of the β_1 peak along with a shift to lower temperature. At higher Zn coverages this peak decreased in intensity and split into several small peaks between 200 and 300 K. In contrast, the β_2-H_2 peak

dx.doi.org/10.1021/jp400798q | J. Phys. Chem. C 2013, 117, 6692−6701

remained at 450 K, peaked in intensity for 0.3 ML of Zn, and then decreased monotonically with increasing Zn coverage.

To provide comparison data for the reaction of methanol on a Zn surface, a methanol TPD experiment was also performed using a Pt(111) sample covered with a 3 ML of Zn film. As shown in Figure 5, the Zn surface is unreactive toward CH_3OH

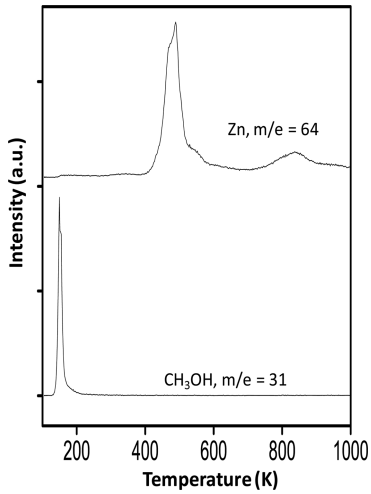

Figure 5. TPD spectra obtained following 2 L of CH_3OH dose at 100 K on freshly deposited 3 ML of Zn film on Pt(111).

and this molecule adsorbs reversibly, desorbing intact at 150 K. The Zn desorption spectrum is also included in this figure. On the basis of previous results reported by Rodriguez et al.,[34] the large Zn peak at 490 K can be attributed to desorption of the Zn multilayers, while the smaller peak at 850 K is associated with the PtZn alloy which was formed during the TPD run.

Since CH_2O was one of the primary reaction products during the reaction of CH_3OH on Zn/Pt(111), TPD spectra for CH_2O-dosed surfaces (1 L) were also obtained and are shown in Figure 6. On clean Pt(111), CH_2O primarily decomposes to form CO and H_2 which desorb at 450 and 325 K, respectively. A small CH_2O peak is also apparent at 280 K. These results align well with those reported in the literature for reaction of formaldehyde on Pt(111).[47] Deposition of 0.3 ML of Zn prior to the CH_2O dose resulted in significant changes in the TPD results, including the appearance of a larger, second CH_2O peak at 438 K, a second H_2 peak at 450 K, and the splitting of the CO peak into the α_1 (405 K) and α_2 (497 K) states that were also observed for the CH_3OH-dosed surface. The two separate CH_2O peaks persist for higher Zn coverages with the intensity of the low-temperature peak increasing at the expense of that at high-temperature. The trends in the CO and H_2 desorption spectra at higher Zn coverages were similar to those observed for the methanol-dosed surface.

HREELS was used to identify stable intermediates that were formed by the reaction of CH_3OH on the Zn/Pt(111) surface. Figure 7 shows the evolution of the HREEL vibrational

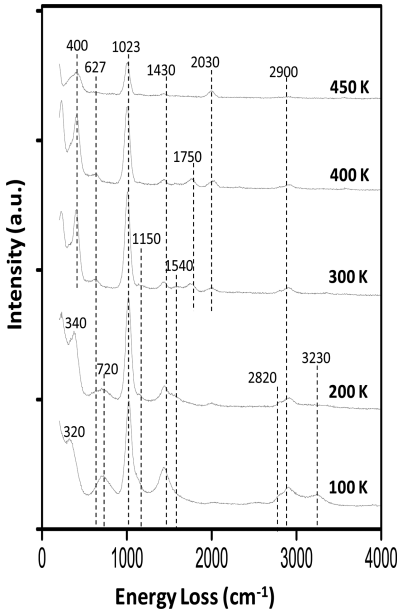

Figure 7. HREEL spectra for 0.4 ML of Zn/Pt(111) dosed with 2 L of CH_3OH at 100 K and upon annealing progressively to higher temperatures.

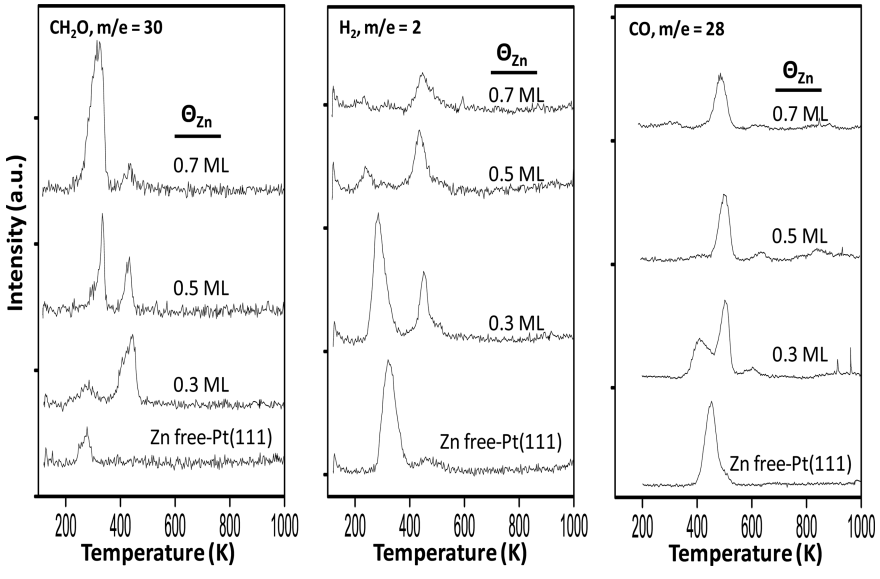

Figure 6. TPD spectra obtained following a 1 L dose of CH_2O at 100 K on Zn/Pt(111) as a function of Zn coverage.

dx.doi.org/10.1021/jp400798q | J. Phys. Chem. C 2013, 117, 6692−6701

Table 1. Vibrational Mode Assignments for CH_3OH-Dosed Zn/Pt(111)

	frequency, cm^{-1}					
mode	crystalline CH_3OH[48] at 93 K	~0.4 ML of Zn/Pt(111) at 100 K	~0.4 ML of Zn/Pt(111) at 200 K	~0.4 ML of Zn/Pt(111) at 300 K	~0.4 ML of Zn/Pt(111) at 400 K	~0.4 ML of Zn/Pt(111) at 450 K
ν(OH)	3235	3230	3230	–	–	–
$\nu_{as}(CH_3)$, $\nu_{as}(CH_2)$	2955	2900	2900	2900	2900	(2900)
$\nu_s(CH_3)$, $\nu_s(CH_2)$	2829	2820	2820	–	–	–
$\delta(CH_3)$, $\delta(CH_2)$	1445	1430	1430	1430	1430	(1430)
$\rho(CH_3)$	1187	1150	1150	–	–	–
ν(CO), CH_3OH	1038	1023	1023	1007	1007	990
ν(CO), η^1-CH_2O		–	–	1750	1750	–
ν(CO), CO		–	–	2030	2030	2030
δ(COH)	1490	(1540)	1540	1540	–	–
γ(OH)	740	720	720	–	–	–
δ(M–O)		–	–	627	627	627
ν(Zn–O)		–	–	400	400	400
ν(Pt–O)		(320)	(340)	–	–	(340)

spectrum for a 0.4 ML of Zn/Pt(111) dosed with 2 L of CH_3OH at 100 K, as a function of the annealing temperature. The peak positions and mode assignments for the spectra are tabulated in Table 1. For comparison, the peak positions in the IR spectrum of CH_3OH are also included in the table.[48] After dosing at 100 K, the sample is covered with multilayers of CH_3OH, and as shown in the table, there is good agreement between the vibrational spectrum of the adsorbed multilayer CH_3OH film and that reported in the literature for crystalline methanol.

Annealing the sample to 200 K produced only minor changes in the HREEL spectrum. As shown in the TPD results in Figure 4, this temperature is sufficient to desorb the weakly bound CH_3OH multilayers. Thus, the persistence of the vibrational modes indicative of OH groups in this HREEL spectrum (i.e., ν(OH), ~3230 cm^{-1}; δ(COH), ~1500 cm^{-1}; and γ(OH), ~720 cm^{-1}) demonstrates that CH_3OH adsorbs molecularly on the 0.4 ML of Zn/Pt(111) surface at this temperature.

Upon heating to 300 K, the peaks indicative of the OH groups nearly disappear and the intense ν(CO) peak shifts from 1023 to 1007 cm^{-1}. New peaks also emerge at 400 and 627 cm^{-1} which are at positions typically observed for the metal–oxygen stretching and deformation modes, respectively, of alkoxides adsorbed on metal surfaces.[38,49−53] All of these factors point to O–H bond cleavage in the adsorbed methanol to form methoxide intermediates. Whether these intermediates are bound to Pt or Zn sites will be addressed in the Discussion. Additional changes in the spectrum include the appearance of small peaks at 1750 and 2030 cm^{-1}, indicating the formation of additional surface intermediates. The peak at 1750 cm^{-1} is at a frequency that is characteristic of the ν(CO) mode of H_2CO adsorbed on transition metals in an η^1 configuration where bonding to the surface occurs via the oxygen atom. The presence of this species demonstrates that C–H bond scission in the adsorbed methoxide intermediates has started to occur by 300 K. The peak at 2030 cm^{-1} is readily assigned to CO adsorbed atop Pt sites[38,43,54] which is either the product of complete dehydrogenation of a small fraction of the adsorbed methoxides or, perhaps due to the adsorption of a small amount of CO from the chamber background. Heating to 400 K and then 450 K caused all the peaks associated with adsorbed $-OCH_3$ and η^1-H_2CO to decrease in intensity with a concomitant increase in the intensity of the ν(CO) peak for adsorbed CO. A new peak also emerges at 340 cm^{-1} which can be assigned to the ν(Pt–C) mode of the adsorbed CO.

DISCUSSION

The results of this study show that the reactivity of Pt(111) toward methanol is modified by both Zn adatoms and Zn atoms incorporated into the near surface region. Consistent with the literature,[38,40,51,55,56] we observed that the Pt(111) surface had relatively low reactivity toward molecular methanol, with a low temperature decomposition pathway to form CO occurring primarily at defect sites. Substituting Zn into the surface and near surface layers had only a minor effect on this pathway causing, as shown in Figure 2, a slight increase in methanol dehydrogenation activity when <0.6 ML of Zn were used during alloy synthesis, and little to no effect for higher Zn coverages. The data in Figure 2 also show that the CO desorption temperature decreases slightly with the increasing Zn concentration which is consistent with previous studies of the interaction of CO with PtZn and PdZn alloy surfaces.[24,34,35] Note that a previous LEIS study of PtZn/Pt(111) surfaces formed in the same manner as those used here (i.e., vapor deposition of Zn followed by annealing to 600 K) demonstrated that the concentration of Zn in the surface layer is less than 5 at. %. Thus, it is perhaps not surprising that alloying caused only subtle changes in the surface reactivity. Much more dramatic effects were observed when the Zn was present in the form of an adatom on the Pt(111) surface. As shown in Figure 3, Zn adatoms stabilize adsorbed CO by ~12 kJ/mol, causing a 50 K increase in the CO desorption temperature. This is an interesting result since it is opposite to what is observed on PtZn alloy surfaces, where as noted above, CO is destabilized relative to clean Pt(111). The decrease in the amount of adsorbed CO for a constant CO dose with increasing Zn adatom coverage demonstrates that CO remains bonded to Pt sites and does not adsorb directly on the Zn. The observation that CO interacts only weakly with Zn is consistent with previous studies of the adsorption of CO on Zn

dx.doi.org/10.1021/jp400798q | J. Phys. Chem. C 2013, 117, 6692−6701

surfaces.[44−46] The trend in the CO TPD peak position with Zn coverage also suggests that stabilization of adsorbed CO is limited to Pt sites in close proximity to a Zn adatom.

As shown by the TPD data in Figure 4, complex behavior is observed for the reaction of CH_3OH on the Zn/Pt(111) surfaces. Adding only 0.1 ML of Zn adatoms caused the molecular methanol desorption peak to shift from 190 to 220 K and decrease significantly in intensity, along with a concomitant increase in the amount of CO and H_2 produced at higher temperatures. Note that the HREELS data in Figure 7 shows that for CH_3OH-dosed 0.4 ML of Zn/Pt(111), methanol remains largely intact at 200 K. While it is tempting to assign the stabilized form of molecular methanol to species adsorbed on Zn sites, the fact that this species is not observed for the high coverage Zn/Pt(111) samples which also exhibit low dehydrogenation activity argues against this. The methanol TPD data obtained from 3 ML of Zn/Pt(111) (Figure 5), which shows that methanol desorbs below 200 K and is the sole product, further supports the hypothesis that intact methanol does not adsorb strongly on Zn sites. Thus, it appears that the Zn adatoms stabilize molecular methanol that is adsorbed on nearby Pt sites.

The TPD and HREELS data show that O−H bond scission, resulting in the formation of adsorbed methoxide groups, competes with direct desorption of the Zn-stabilized form of adsorbed molecular methanol. These methoxide groups undergo C−H bond scission producing CH_2O and ultimately CO. From the TPD and HREELS data it is not clear whether the Zn adatoms participate directly in the O−H bond scission reaction to form methoxide groups, or whether they merely serve to stabilize the adsorbed CH_3OH to a sufficiently high temperature such that O−H scission can occur on the exposed portions of the Pt(111) surface. To provide additional insight into the role of the Zn adatoms in this reaction, XP-spectra of a 0.4 ML of Zn/Pt(111) sample dosed 2 L of CH_3OH were collected as a function of temperature and are depicted in Figure 8. Since the Zn(2p) peaks are not very sensitive to changes in electron density, e.g. there is only a ∼0.2 eV shift between Zn^0 and Zn^{2+},[57] we instead collected spectra for the X-ray induced $L_3M_{45}M_{45}$ Auger peak which is more sensitive to the Zn chemical state. As shown in Figure 8, the freshly deposited Zn on Pt(111) exists in the metallic state with the $L_3M_{45}M_{45}$ peak at the expected energy of 992.5 eV.[58,59] Note that following CH_3OH adsorption at 100 K, the center of the Zn $L_3M_{45}M_{45}$ peak shifts slightly to lower kinetic energy and upon heating to 200 K it is centered at 991.5 eV. This peak position is consistent with that reported in the literature for Zn^{2+}.[58,59] The peak position remains fixed upon heating to 300 K, but shifts back to 992.5 eV upon heating to 600 K, which is above the desorption temperature for all of the reaction products. A similar experiment was performed for a 0.4 ML PtZn/Pt(111) alloy surface and the $L_3M_{45}M_{45}$ peak position was found to remain fixed at 992.5 eV. Since oxygen is electron withdrawing relative to Zn, the results of these XPS experiments are consistent with at least some of the methoxide groups formed on the Zn/Pt(111) surface being bonded to the Zn adatoms.

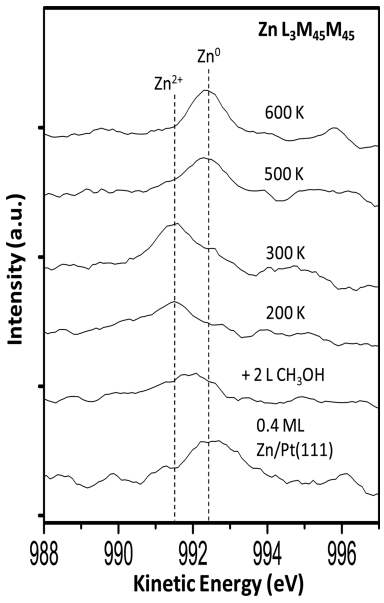

Figure 8. X-ray induced Zn($L_3M_{45}M_{45}$) Auger spectra obtained from 0.4 ML of Zn/Pt(111) dosed with 2 L of CH_3OH dose at 100 K and upon annealing progressively to higher temperatures.

The data provide some hints to the reaction pathways for the Zn−adatom bound methoxide groups. Note that during TPD with methanol-dosed Zn/Pt(111) both the α_1 and α_2 CO desorption peaks are observed. As described above, our data indicates that these peaks arise from CO adsorbed on Pt sites. Thus, there are no CO peaks that appear to originate from reaction of the Zn-bound methoxides. There is some evidence, however, that suggests that the CH_2O that desorbs at 438 K during CH_3OH TPD with the Zn/Pt(111) surfaces is produced via dehydrogenation of the Zn-bond methoxides. Based on HREELS data, Sen and Rao have reported that methoxide species produced by the reaction of methanol on O_2 predosed Zn(0001) at 80 K undergo dehydrogenation to form CH_2O at ∼300 K as indicated by the presence of a ν(CO) mode at 1750 cm^{-1} which is indicative of η^1-CH_2O.[60] Note that this peak is also observed in the HREEL spectrum of the methanol-dosed Zn/Pt(111) surface after heating to 300 and 400 K (see Figure 7). The H_2 peaks between 195 and 300 K appear to be reaction limited and associated with the dehydrogenation of these Zn-bound methoxide groups.

According to this scenario the CH_2O TPD peak at 438 K must be desorption limited. Note that on clean Pt(111), CH_2O undergoes complete dehydrogenation to CO and H below 250 K.[47,61] In contrast, upon deposition of ∼0.3 ML of Zn prior to CH_2O dosage, a CH_2O desorption peak is observed at 438 K (see Figure 6). Thus, the Zn adatoms do prevent dehydrogenation of at least a portion of the adsorbed CH_2O. The interpretation of the CH_2O TPD data is complicated, however, by the fact that a second, lower-temperature CH_2O peak is also observed at 320 K. This low-temperature peak grows in intensity at the expense of the high-temperature peak with increasing Zn coverage. We propose that this peak results from the rapid depolymerization of paraformaldehyde formed by reaction of the adsorbed formaldehyde. Polymerization of adsorbed formaldehyde is known to occur on metal surfaces[23,47,49,62] including Zn as reported by Sen and Rao.[60] It is also not surprising that this species would not be formed at low Zn coverages where the Zn would be in the form of isolated sites. Note that CO and H_2 are also produced during CH_2O TPD on Zn/Pt(111). The fact that the amount of these products decreases with increasing Zn coverage indicates that they result from reactions taking place on the exposed Pt sites.

dx.doi.org/10.1021/jp400798q | J. Phys. Chem. C 2013, 117, 6692−6701

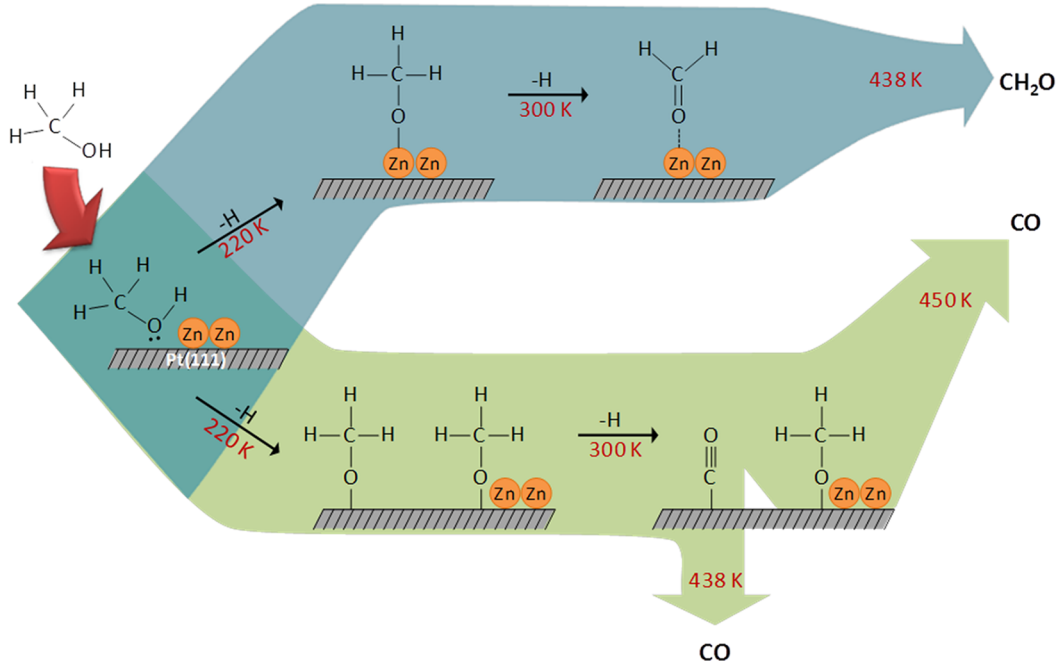

Figure 9. Proposed pathways for reaction of CH_3OH on Zn/Pt(111) surfaces.

Figure 9 summarizes the pathways that were observed for reaction of methanol on the Zn/Pt(111) surfaces. The upper branch in this diagram shows the pathways for methoxide groups bound to the Zn adatoms. In accordance with the analysis presented above, CH_3OH adsorbed on Pt sites adjacent to the Zn adatoms are stabilized relative to Zn-free Pt(111) and undergo O−H bond scission to form methoxide (CH_3O−) groups upon annealing to 200 K, a portion of which are bound to the Zn adatoms. These Zn-bound methoxides undergo C−H bond scission to form adsorbed η^1-CH_2O at ∼300 K. These formaldehyde intermediates desorb upon heating to 438 K.

As noted above, the temperatures for the CO desorption peaks obtained from the CH_3OH-dosed Zn/Pt(111) surfaces are consistent with those for CO adsorbed on Pt sites. This suggests that in addition to the pathway that produces formaldehyde from Zn-bond methoxides, there must be additional pathways that involve intermediates adsorbed on the exposed portions of the Pt(111) surface. We therefore propose that in addition to Zn-bound methoxides, the Zn adatoms also facilitate the formation of Pt-bound methoxides from adsorbed methanol. The HREEL spectra obtained from methanol-dosed Zn/Pt(111) (Figure 7) show the appearance of a ν(CO) mode at 2030 cm^{-1} associated with adsorbed CO upon annealing the sample to 300 K. This indicates that at least a portion of these adsorbed methoxide groups undergo dehydrogenation at or slightly below this temperature. Allowing for surface diffusion of CO, this pathway would populate both the α_1 (Pt(111)) and α_2 (Zn-modified Pt(111)) CO adsorption sites.

The HREEL data also show that some methoxide groups remain intact up to 450 K. The presence of a desorption-limited H_2 peak at 450 K from Zn/Pt(111) is also consistent with this observation. This result is more difficult to rationalize since dehydrogenation of methoxides adsorbed on both the Zn adatoms and Zn-free portions of the Pt(111) surface commences well below this temperature. We speculate that these more thermally stable methoxide intermediates are adsorbed on the Pt sites adjacent to the Zn adatoms, although additional study is needed to confirm this. Dehydrogenation of these methoxide intermediates would populate only α_2 CO adsorption sites. These proposed pathways for the reaction of methoxide groups on the exposed Pt portions of the surface are summarized by the lower branches in the reaction pathway diagram in Figure 9.

As shown in Figure 9, we ascribe the production of formaldehyde to dehydrogenation of Zn-bound methoxides, and the production of both the α_1 and α_2 CO to dehydrogenation of methoxide groups bound to Zn-free and Zn-modified Pt sites. A plot of the C_1 TPD product yield obtained from 2 L of CH_3OH-dosed Zn/Pt(111) surfaces as a function of Zn adatom coverage shown in Figure 10, provides

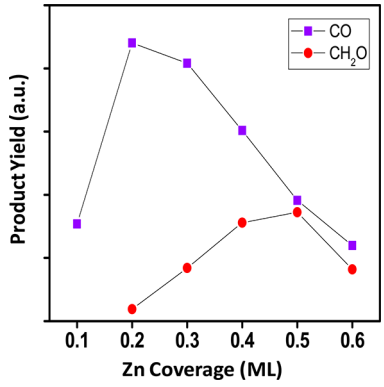

Figure 10. C_1 product yield obtained following CH_3OH TPD on Zn adatoms/Pt(111) as a function of Zn coverage.

additional support for this conclusion. Note that addition of 0.2 ML of Zn adatoms causes a large increase in the CO product yield and is consistent with the proposed reaction pathway discussed above, where the dehydrogenation of methanol to methoxide occurs only on the Zn-modified Pt sites. Apparently relatively few such sites are needed in order to populate the

dx.doi.org/10.1021/jp400798q | J. Phys. Chem. C 2013, 117, 6692−6701

surface with methoxide groups. A linear decline in CO yield is observed, however, upon increasing the Zn coverage above 0.2 ML with extrapolation of the data indicating that the CO product yield would be near zero for 1 ML of Zn coverage. This trend is consistent with the CO being produced on the exposed portions of the Pt(111) surface. In contrast to CO, the CH_2O yield initially increases nearly linearly with Zn adatom coverage, for coverages up to 0.5 ML, at which point it decreases with further increases in Zn coverage. The initial linear increase with Zn coverage supports the conclusion that the CH_2O product results from a reaction taking place on the Zn sites. The decrease at high Zn coverages can be attributed to loss of the Pt−Zn interfacial sites which are necessary for the initial O−H bond scission step which forms the methoxide groups.

Since under typical SRM reaction conditions, the ratio of Pt to Zn in Pt/ZnO catalysts is higher than that what was accessible here for the PtZn/Pt(111) samples, one must be cautious when attempting to extrapolate the insights obtained in this study to real catalysts. As noted above, based on our previous characterization studies,[35] the Zn concentration in the outermost layer of the PtZn/Pt(111) samples was less than 5 at. %. The primary effect on reactivity of the Zn in these samples was to provide sites for dissociative adsorption of CH_3OH. The reaction of the resulting methoxide species, however, was similar to that on Zn-free Pt(111) with complete dehydrogenation CO and H_2 taking place. This observation aligns well with the SRM studies over analogous unsupported Pd−Zn bimetallic catalysts reported by Halevi et al.[21] in which it was found that addition of a small amount of Zn to Pd had little effect on the SRM selectivity. High selectivity to CO_2 and H_2 was obtained only for catalysts where the Pd:Zn ratio was close to 1:1. This corresponds to the formation of the thermodynamically stable PdZn intermetallic compound.[21,26,63,64]

There is some evidence in the literature, however, that suggests that excess Zn is required in PtZn and PdZn catalysts for high CO_2/H_2 selectivity.[26,27,65] For example, Friedrich et al.[65] have reported that the selectivity to CO_2 during SRM shifts from ∼10% to over 98% upon increasing the Zn content in unsupported PdZn alloys from 48 to 54%. While this result is consistent with the need to form the 1:1 intermetallic compound to obtain high selectivity, they also observed by XPS that a distinguishing characteristic of the highly CO_2 selective catalysts was the presence of a small amount of excess Zn that was not incorporated into the alloy. Their XPS measurements were made in situ with the sample exposed to 0.2 mbar of 2:1 H_2O:CH_3OH mixture and under these conditions the excess Zn was present in the form of a surface ZnO species. They concluded that only samples rich in Zn exhibit the extraordinarily high selectivity to CO_2. Our results indicate that one possible role of excess surface Zn is to provide sites that stabilize adsorbed CH_2O from further dehydrogenation allowing them to react with hydroxyl groups to form dioxymethylene and formate which are likely intermediates in reaction pathways which produce CO_2 rather than CO.[20,21,66] This conclusion is also in accordance with that of Iwasa and Takezawa who propose a similar role for Zn in both PtZn and PdZn SRM catalysts.[6,18,20]

CONCLUSIONS

The results of this study provide new insights into the role of Zn in altering the reactivity of Pt(111) surfaces toward methanol. The dehydrogenation of adsorbed methoxy groups (CH_3O−) was found to be significantly inhibited through the presence of Zn adatoms on Pt surfaces, as demonstrated by the production of formaldehyde as a primary product from methanol-dosed Zn/Pt(111). This role of Zn is similar to that reported previously for Zn-modified Pd where increased barriers for C−H bond scission in adsorbed methoxide have also been observed.

AUTHOR INFORMATION

Corresponding Author

*E-mail: (J.M.V.) vohs@seas.upenn.edu.

Notes

The authors declare no competing financial interest.

ACKNOWLEDGMENTS

Funding for this study was provided by the U.S. Department of Energy (Grant No. DE-FG02-04ER15605).

REFERENCES

(1) Ghenciu, A. F. Review of fuel processing catalysts for hydrogen production in PEM fuel cell systems. *Curr. Opin. Solid State Mater.* **2002**, *6*, 389−399.

(2) Song, C. S. Fuel processing for low-temperature and high-temperature fuel cells - Challenges, and opportunities for sustainable development in the 21st century. *Catal. Today* **2002**, *77*, 17−49.

(3) Armor, J. N. The multiple roles for catalysis in the production of H_2. *Appl. Catal., A* **1999**, *176*, 159−176.

(4) Bharadwaj, S. S.; Schmidt, L. D. Catalytic Partial Oxidation of Natural-Gas to Syngas. *Fuel Process. Technol.* **1995**, *42*, 109−127.

(5) Sa, S.; Silva, H.; Brandao, L.; Sousa, J. M.; Mendes, A. Catalysts for methanol steam reforming-A review. *Appl. Catal., B* **2010**, *99*, 43−57.

(6) Iwasa, N.; Yoshikawa, M.; Nomura, W.; Arai, M. Transformation of methanol in the presence of steam and oxygen over ZnO-supported transition metal catalysts under stream reforming conditions. *Appl. Catal., A* **2005**, *292*, 215−222.

(7) Suwa, Y.; Ito, S. I.; Kameoka, S.; Tomishige, K.; Kunimori, K. Comparative study between Zn-Pd/C and Pd/ZnO catalysts for steam reforming of methanol. *Appl. Catal., A* **2004**, *267*, 9−16.

(8) Fottinger, K.; van Bokhoven, J. A.; Nachtegaal, M.; Rupprechter, G. Dynamic Structure of a Working Methanol Steam Reforming Catalyst: In Situ Quick-EXAFS on Pd/ZnO Nanoparticles. *J. Phys. Chem. Lett.* **2011**, *2*, 428−433.

(9) Lebarbier, V. M.; Karim, A. M.; Engelhard, M. H.; Wu, Y.; Xu, B. Q.; Petersen, E. J.; Datye, A. K.; Wang, Y. The Effect of Zinc Addition on the Oxidation State of Cobalt in Co/ZrO_2 Catalysts. *Chemsuschem* **2011**, *4*, 1679−1684.

(10) Song, H.; Zhang, L. Z.; Watson, R. B.; Braden, D.; Ozkan, U. S. Investigation of bio- ethanol steam reforming over cobalt-based catalysts. *Catal. Today* **2007**, *129*, 346−354.

(11) Llorca, J.; Homs, N.; Sales, J.; de la Piscina, P. R. Efficient production of hydrogen over supported cobalt catalysts from ethanol steam reforming. *J. Catal.* **2002**, *209*, 306−317.

(12) Martono, E.; Vohs, J. M. Support effects in cobalt-based ethanol steam reforming catalysts: Reaction of ethanol on Co/CeO_2/YSZ(100) model catalysts. *J. Catal.* **2012**, *291*, 79−86.

(13) Agrell, J.; Boutonnet, M.; Fierro, J. L. G. Production of hydrogen from methanol over binary Cu/ZnO catalysts - Part II. Catalytic activity and reaction pathways. *Appl. Catal., A* **2003**, *253*, 213−223.

(14) Agrell, J.; Birgersson, H.; Boutonnet, M.; Melian-Cabrera, I.; Navarro, R. M.; Fierro, J. L. G. Production of hydrogen from methanol over Cu/ZnO catalysts promoted by ZrO_2 and Al_2O_3. *J. Catal.* **2003**, *219*, 389−403.

(15) Peters, R.; Dusterwald, H. G.; Hohlein, B. Investigation of a methanol reformer concept considering the particular impact of

dynamics and long-term stability for use in a fuel- cell-powered passenger car. *J. Power Sources* **2000**, *86*, 507−514.
(16) Raimondi, F.; Schnyder, B.; Kotz, R.; Schelldorfer, R.; Jung, T.; Wambach, J.; Wokaun, A. Structural changes of model Cu/ZnO catalysts during exposure to methanol reforming conditions. *Surf. Sci.* **2003**, *532*, 383−389.
(17) Twigg, M. V.; Spencer, M. S. Deactivation of copper metal catalysts for methanol decomposition, methanol steam reforming and methanol synthesis. *Top. Catal.* **2003**, *22*, 191−203.
(18) Takezawa, N.; Iwasa, N. Steam reforming and dehydrogenation of methanol: Difference in the catalytic functions of copper and group VIII metals. *Catal. Today* **1997**, *36*, 45−56.
(19) Iwasa, N.; Mayanagi, T.; Ogawa, N.; Sakata, K.; Takezawa, N. New catalytic functions of Pd-Zn, Pd-Ga, Pd-In, Pt-Zn, Pt-Ga and Pt-In alloys in the conversions of methanol. *Catal. Lett.* **1998**, *54*, 119−123.
(20) Iwasa, N.; Takezawa, N. New supported Pd and Pt alloy catalysts for steam reforming and dehydrogenation of methanol. *Top. Catal.* **2003**, *22*, 215−224.
(21) Halevi, B.; Peterson, E. J.; Roy, A.; DeLariva, A.; Jeroro, E.; Gao, F.; Wang, Y.; Vohs, J. M.; Kiefer, B.; Kunkes, E.; et al. Catalytic reactivity of face centered cubic PdZn alpha for the steam reforming of methanol. *J. Catal.* **2012**, *291*, 44−54.
(22) Weilach, C.; Kozlov, S. M.; Holzapfel, H. H.; Fottinger, K.; Neyman, K. M.; Rupprechter, G. Geometric Arrangement of Components in Bimetallic PdZn/Pd(111) Surfaces Modified by CO Adsorption: A Combined Study by Density Functional Calculations, Polarization-Modulated Infrared Reflection Absorption Spectroscopy, and Temperature- Programmed Desorption. *J. Phys. Chem. C* **2012**, *116*, 18768−18778.
(23) Jeroro, E.; Vohs, J. M. Zn modification of the reactivity of Pd(111) toward methanol and formaldehyde. *J. Am. Chem. Soc.* **2008**, *130*, 10199−10207.
(24) Jeroro, E.; Lebarbler, V.; Datye, A.; Wang, Y.; Vohs, J. M. Interaction of CO with surface PdZn alloys. *Surf. Sci.* **2007**, *601*, 5546−5554.
(25) Nozawa, K.; Endo, N.; Kameoka, S.; Tsai, A. P.; Ishii, Y. Catalytic Properties Dominated by Electronic Structures in PdZn, NiZn, and PtZn Intermetallic Compounds. *J. Phys. Soc. Jpn.* **2011**, *80*.
(26) Rameshan, C.; Stadlmayr, W.; Weilach, C.; Penner, S.; Lorenz, H.; Havecker, M.; Blume, R.; Rocha, T.; Teschner, D.; Knop-Gericke, A.; et al. Subsurface-Controlled CO_2 Selectivity of PdZn Near-Surface Alloys in H_2 Generation by Methanol Steam Reforming. *Angew. Chem., Int. Ed.* **2010**, *49*, 3224−3227.
(27) Zhang, Q. L.; Farrauto, R. J. A PdZn catalyst supported on stabilized ceria for stoichiometric methanol steam reforming and hydrogen production. *Appl. Catal., A* **2011**, *395*, 64−70.
(28) Rodriguez, J. A.; Kuhn, M. Interaction of zinc with transition-metal surfaces: Electronic and chemical perturbations induced by bimetallic bonding. *J. Phys. Chem.* **1996**, *100*, 381−389.
(29) Lin, S.; Xie, D. Q.; Guo, H. Pathways of Methanol Steam Reforming on PdZn and Comparison with Cu. *J. Phys. Chem. C* **2011**, *115*, 20583−20589.
(30) Rameshan, C.; Weilach, C.; Stadlmayr, W.; Penner, S.; Lorenz, H.; Havecker, M.; Blume, R.; Rocha, T.; Teschner, D.; Knop-Gericke, A.; et al. Steam reforming of methanol on PdZn near-surface alloys on Pd(111) and Pd foil studied by in-situ XPS, LEIS, and PM-IRAS. *J. Catal.* **2010**, *276*, 101−113.
(31) Stadlmayr, W.; Rameshan, C.; Weilach, C.; Lorenz, H.; Havecker, M.; Blume, R.; Rocha, T.; Teschner, D.; Knop-Gericke, A.; Zemlyanov, D.; et al. Temperature-Induced Modifications of PdZn Layers on Pd(111). *J. Phys. Chem. C* **2010**, *114*, 10850−10856.
(32) Neyman, K. M.; Lim, K. H.; Chen, Z. X.; Moskaleva, L. V.; Bayer, A.; Reindl, A.; Borgmann, D.; Denecke, R.; Steinruck, H. P.; Rosch, N. Microscopic models of PdZn alloy catalysts: structure and reactivity in methanol decomposition. *Phys. Chem. Chem. Phys.* **2007**, *9*, 3470−3482.
(33) Tsai, A. P.; Kameoka, S.; Ishii, Y. PdZn=Cu: Can an intermetallic compound replace an element? *J. Phys. Soc. Jpn.* **2004**, *73*, 3270−3273.
(34) Rodriguez, J. A.; Kuhn, M. Chemical and Electronic-Properties of Pt in Bimetallic Surfaces - Photoemission and Co-Chemisorption Studies for Zn/Pt(111). *J. Chem. Phys.* **1995**, *102*, 4279−4289.
(35) Ho, C. S.; Martono, E.; Roszell, J. P.; Vohs, J. M.; Koel, B. E. Low-energy Alkali Ion Scattering and X-ray Photoelectron Diffraction Studies of the Structure of PtZn/Pt(111) Bimetallic Surfaces. Submitted for publication.
(36) Rodriguez, J. A. Electronic and chemical properties of Pt, Pd, and Ni in bimetallic surfaces. *Surf. Sci.* **1996**, *345*, 347−362.
(37) Weirum, G.; Kratzer, M.; Koch, H. P.; Tamtogl, A.; Killmann, J.; Bako, I.; Winkler, A.; Surnev, S.; Netzer, F. P.; Schennach, R. Growth and Desorption Kinetics of Ultrathin Zn Layers on Pd(111). *J. Phys. Chem. C* **2009**, *113*, 9788−9796.
(38) Skoplyak, O.; Menning, C. A.; Barteau, M. A.; Chen, J. G. G. Experimental and theoretical study of reactivity trends for methanol on Co/Pt(111) and Ni/Pt(111) bimetallic surfaces. *J. Chem. Phys.* **2007**, *127*.
(39) Akhter, S.; White, J. M. A Static SIMS/TPD Study of the Kinetics of Methoxy Formation and Decomposition on O/Pt(111). *Surf. Sci.* **1986**, *167*, 101−126.
(40) Gibson, K. D.; Dubois, L. H. Step Effects in the Thermal-Decomposition of Methanol on Pt(111). *Surf. Sci.* **1990**, *233*, 59−64.
(41) Hayden, B. E.; Kretzschmar, K.; Bradshaw, A. M.; Greenler, R. G. An Infrared Study of the Adsorption of CO on a Stepped Platinum Surface. *Surf. Sci.* **1985**, *149*, 394−406.
(42) Skoplyak, O.; Menning, C. A.; Barteau, M. A.; Chen, J. G. G. Reforming of Oxygenates for H_2 Production on 3d/Pt(111) Bimetallic Surfaces. *Top. Catal.* **2008**, *51*, 49−59.
(43) Steininger, H.; Lehwald, S.; Ibach, H. On the Adsorption of CO on Pt(111). *Surf. Sci.* **1982**, *123*, 264−282.
(44) Carley, A. F.; Roberts, M. W.; Yan, S. The Influence of Preoxidation on the Adsorption of CO at a Zn(0001) Surface - Characterization of a Weakly Chemisorbed Species by XPS and UPS. *Appl. Surf. Sci.* **1990**, *40*, 289−293.
(45) Rodriguez, J. A. The Chemical-Properties of Bimetallic Surfaces - Bonding between CO and Zn on Ru(001). *Surf. Sci.* **1993**, *289*, L584−L590.
(46) Rodriguez, J. A. Interactions in Bimetallic Bonding - Electronic and Chemical-Properties of PdZn Surfaces. *J. Phys. Chem.* **1994**, *98*, 5758−5764.
(47) Henderson, M. A.; Mitchell, G. E.; White, J. M. The Decomposition of Formaldehyde on Pt(111) - a TPD and HREELS Study. *Surf. Sci.* **1987**, *188*, 206−218.
(48) Falk, M.; Whalley, E. Infrared Spectra of Methanol and Deuterated Methanols in Gas, Liquid, and Solid Phases. *J. Chem. Phys.* **1961**, *34*, 1554.
(49) Houtman, C.; Barteau, M. A. Reactions of Methanol on Rh(111) and Rh(111)-(2 × 2)O Surfaces - Spectroscopic Identification of Adsorbed Methoxide and η^1-Formaldehyde. *Langmuir* **1990**, *6*, 1558−1566.
(50) Christmann, K.; Demuth, J. E. The Adsorption and Reaction of Methanol on Pd(100) 0.1. Chemisorption and Condensation. *J. Chem. Phys.* **1982**, *76*, 6308−6317.
(51) Sexton, B. A. Methanol Decomposition on Platinum (111). *Surf. Sci.* **1981**, *102*, 271−281.
(52) Bare, S. R.; Stroscio, J. A.; Ho, W. Characterization of the Adsorption and Decomposition of Methanol on Ni(110). *Surf. Sci.* **1985**, *150*, 399−418.
(53) Wang, J.; Deangelis, M. A.; Zaikos, D.; Setiadi, M.; Masel, R. I. Methanol Oxidation on (2 × 1)Pt(110) - Formaldehyde on a Stepped Surface. *Surf. Sci.* **1994**, *318*, 307−320.
(54) Baro, A. M.; Ibach, H. New Study of CO Adsorption at Low-Temperature (90 K) on Pt(111) by EELS. *J. Chem. Phys.* **1979**, *71*, 4812−4816.
(55) Greeley, J.; Mavrikakis, M. A first-principles study of methanol decomposition on Pt(111). *J. Am. Chem. Soc.* **2002**, *124*, 7193−7201.

(56) Greeley, J.; Mavrikakis, M. Competitive paths for methanol decomposition on Pt(111). *J. Am. Chem. Soc.* **2004**, *126*, 3910−3919.
(57) Wagner, C. D.; Riggs, W. M.; Davis, B. H.; Moulder, J. F.; Muilenberg, G. E. *Handbook of X-Ray Photoelectron Spectroscopy*; Perkin-Elmer: Eden Prairie, MN, 1979.
(58) Rodriguez, J. A. Chemical-Properties of Bimetallic Surfaces - the Reaction of O_2 and NO_2 with Zn on Ru(001). *J. Phys. Chem.* **1993**, *97*, 6509−6517.
(59) Leighton, C. A.; Swift, A. J.; Vickerman, J. C. Further Characterization of Pd Deposited on an Extensively Oxidized Zn(001) Support. *Surf. Sci.* **1991**, *253*, 220−232.
(60) Sen, P.; Rao, C. N. R. An Eels Study of Water, Methanol, Formaldehyde and Formic- Acid Adsorbed on Clean and Oxygen-Covered Zinc(0001) Surfaces. *Surf. Sci.* **1986**, *172*, 269−280.
(61) Abbas, N. M.; Madix, R. J. The Effects of Structured Overlayers of Sulfur on the Kinetics and Mechanism of Simple Reactions on Pt(111) 0.1. Formaldehyde Decomposition. *Appl. Surf. Sci.* **1981**, *7*, 241−275.
(62) Fleck, L. E.; Feehery, W. F.; Plummer, E. W.; Ying, Z. C.; Dai, H. L. Laser-Induced Polymerization of Submonolayer Formaldehyde on Ag(111). *J. Phys. Chem.* **1991**, *95*, 8428−8430.
(63) Miura, A.; Wang, H. S.; Leonard, B. M.; Abruna, H. D.; DiSalvo, F. J. Synthesis of Intermetallic PtZn Nanoparticles by Reaction of Pt Nanoparticles with Zn Vapor and Their Application as Fuel Cell Catalysts. *Chem. Mater.* **2009**, *21*, 2661−2667.
(64) Hsiao, Y. J.; Chang, Y. A.; Ipser, H. Thermodynamics of Nonstoichiometric β-1 PtZn Phase Exhibiting L10 Structure. *J. Electrochem. Soc.* **1977**, *124*, 1235−1239.
(65) Friedrich, M.; Teschner, D.; Knop-Gericke, A.; Armbruster, M. Influence of bulk composition of the intermetallic compound ZnPd on surface composition and methanol steam reforming properties. *J. Catal.* **2012**, *285*, 41−47.
(66) Lin, S.; Xie, D. Q.; Guo, H. First-principles study of the methyl formate pathway of methanol steam reforming on PdZn(111) with comparison to Cu(111). *J. Mol. Catal. A* **2012**, *356*, 165−170.